Periodica Polytechnica
Civil Engineering

x(y) pp. x-x, (year)
https://doi.org/10.3311/PPci.XXXX

RESEARCH ARTICLE

Verification of the Ramberg-Osgood Material Model in Midas GTS NX with the Modeling of Torsional Simple Shear Tests

Zsolt Szilvágyi[1,*] and Richard P. Ray[1]

Abstract

This study focuses on the back analysis of a geotechnical laboratory test with nonlinear finite element modeling using the Ramberg-Osgood material model. This model has been used by several authors recently for performing nonlinear ground response analysis and it has been implemented by Midas into their commercial finite element code Midas GTS NX 2014. The verification of the model for 1D nonlinear site response analysis can be found in the documentation of the software package. In this study Torsional Simple Shear tests were modeled and a comprehensive study was performed to provide verification of the material model for static torsional loading and axisymmetric conditions.

Keywords

Ramberg-Osgood model, Torsional Simple Shear Test, small strain stiffness

[1]Department of Structural and Geotechnical Engineering,
Faculty of Architecture, Civil Engineering and Transport Sciences,
Széchenyi István University
H-9026 Győr, Egyetem sqr. 1, Hungary (e-mail: szilvagyi@sze.hu
ray@sze.hu)

[*] Corresponding author, e-mail: szilvagyi@sze.hu

1 Introduction

Recently the importance of numerical modeling in geotechnical engineering has increased greatly; not only in research, but in everyday practice as well. As a result, geotechnical material models have developed tremendously due to their increased use with ever more complex design projects. While advances in computer technology have made this possible; the many economic and practical advantages of faster and more accurate solutions have made it a reality. The cycle time between research, development, deployment, and design implementation has indeed been reduced from years to months.

Since the deployment cycle has shortened, the process of verification and validation are even more crucial [1]. For geotechnical finite element software, verification is the process of showing that a model or method has been properly implemented in a computer program; while validation makes plausible that a computer model possesses the essential features to analyze a real world problem with results that are representative for the situation. The former is usually done by the software developer and the latter should be done by the user when creating a model. This paper focuses on the verification of the Ramberg-Osgood model in an axisymmetric case for static torsional loading. Results of laboratory tests performed on dry sand samples are used to verify the capabilities of the material model.

2 Small strain stiffness of soils

Many studies have shown that the accurate modeling of stiffness degradation with strain (and stress) is a key aspect in many dynamic as well as static geotechnical numerical calculations (e.g. earthquake vibrations, high speed railway induced vibrations, settlement calculations around retaining walls or tunnels etc.). It has been recognized [2], that soils behave linear-elastically only at very low strains (10^{-6} or 10^{-4}

%) and as the strains (and stresses) increase, the initially constant shear stiffness or small strain stiffness (G_{max} or G_0) decreases gradually, as shown in Fig 1, while the damping or hysteretic behavior becomes more pronounced.

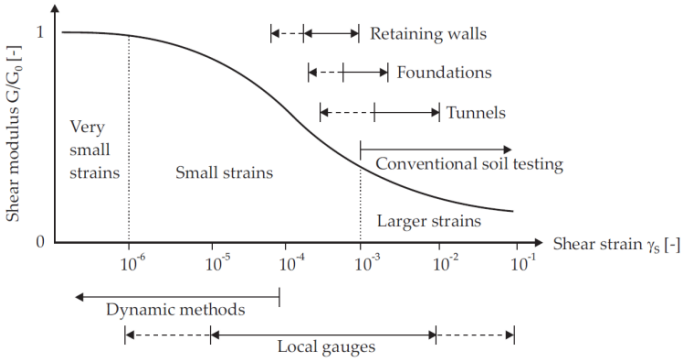

Fig. 1 Stiffness degradation of soil with typical strain ranges after [3]

A detailed discussion is presented in [4] about the small strain stiffness of soils, where first the historical development of elastic theory and the constitutive frameworks for its use in soil modeling is elaborated. Later the author shows how the comprehensive theoretical description of anisotropic elasticity can be simplified for practical calculations regarding soils. It should be emphasized, that beside anisotropy, several other factors have an effect on both the small strain stiffness and stiffness at larger strains.

The most important factors that affect small strain stiffness are:

- void ratio,
- grain properties (grain size and shape),
- effective overburden stress,
- stress history,
- rate of loading,
- structure and fabric of soil,
- discontinuities.

Factors that control the degradation of stiffness at larger strains are:

- strain level,
- loading path (change in effective stress),
- destructuring,
- change in rate of loading.

Some of these factors can be assessed by state of the art laboratory investigations e.g. Torsional Simple Shear (TOSS), Resonant Column, or Bender Element testing. Results of such investigations are used to improve existing material models or create new models which represent more aspects of the real behavior than earlier ones. Numerical models can then be used to investigate some of the factors mentioned above.

3 Formulation of the Ramberg-Osgood model in Midas GTS NX

For cyclic and dynamic modeling the software Midas GTS NX offers several material models which are capable of modeling hysteretic behavior, but only two of them have been implemented for solid and axisymmetric solid elements which are used to model soil layers; the modified Ramberg-Osgood model and the modified Hardin-Drnevich model [5].

The Ramberg-Osgood model [6] was originally introduced for describing stress-strain curves of aluminum-alloy and steel sheets. The model used three parameters to define nonlinear stress-strain behavior, based on initial material stiffness, yield stress, and the rate of transition from linear behavior to full yielding. Later [7] adapted the model to generate nonlinear stress strain behavior and the concurrent shear modulus reduction and damping behavior for soil. The formulation has been modified to various ways [8], [9], and these models are called modified Ramberg-Osgood model. While the expressions are different from the original paper, all modified models are essentially identical. Since then, several authors used the model connected to geotechnical earthquake engineering e.g. [10].

The formulation by Midas uses the main equation for initial loading as:

$$G_0\gamma = \tau(1 + \alpha|\tau|^{\beta}). \tag{1}$$

In (1) G_0 is the initial or small strain stiffness (shear modulus), γ and τ are shear strain and shear stress respectively, α and β are model parameters given by:

$$\alpha = \left(\frac{2}{\gamma_r G_0}\right)^{\beta} \text{ and } \beta = \frac{2\pi h_{max}}{2-\pi h_{max}}. \tag{2}$$

In (2) γ_r is the reference shear strain and h_{max} is the maximum damping constant.

For unloading and reloading the hysteresis curve is as follows:

$$G_0\left(\frac{\gamma \pm \gamma_1}{2}\right) = \left(\frac{\tau \pm \tau_1}{2}\right)\left(1 + \alpha\left(\tau\frac{\tau \pm \tau_1}{2}\right)^{\beta}\right). \tag{3}$$

In (3) γ_1 and τ_1 are the shear strain and stress values at the turnaround point, as shown in Fig. 2.

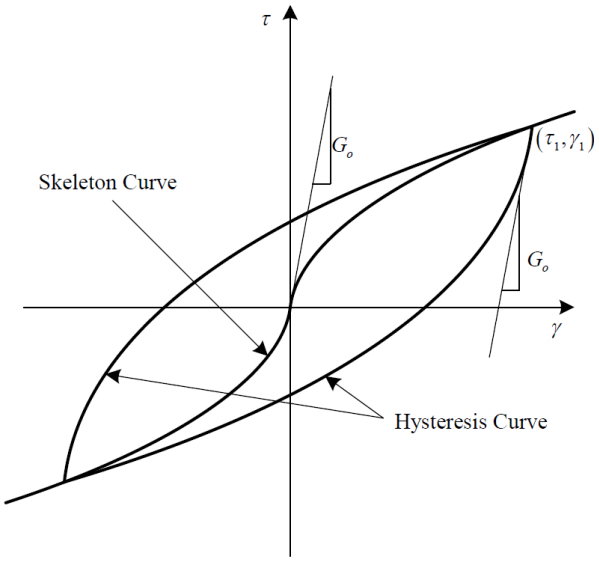

Fig. 2 Hysteresis loop of the Ramberg-Osgood model

4 Torsional Shear and Resonant Column Tests

A combined Resonant Column-Torsional Simple Shear device (RC-TOSS) designed and built by one of the authors, was used for testing [11], [10]. It has been further developed and used in previous studies at SZE [12], [13] and [14]. The benefit of the combined testing is that small strain stiffness G_0 small strain damping, large strain stiffness and damping can be determined by two independent means on the same specimen in the same test. Additionally, arbitrary (earthquake) load histories or resonant and cyclic tests can be performed with an initial static torsional load applied. Both measurements can be performed on the same specimen over a wide range of strains and results can be checked against each other.

For RC testing, the device has a fixed-free configuration with the hollow cylinder (ID=4cm, OD=6cm, L=14cm) sample connected rigidly to a base platen. The loading system, consisting of a top cap, suspension rod, drive head and two neodymium magnets rests on top of the specimen. It is free to rotate without restriction, see Fig. 3.

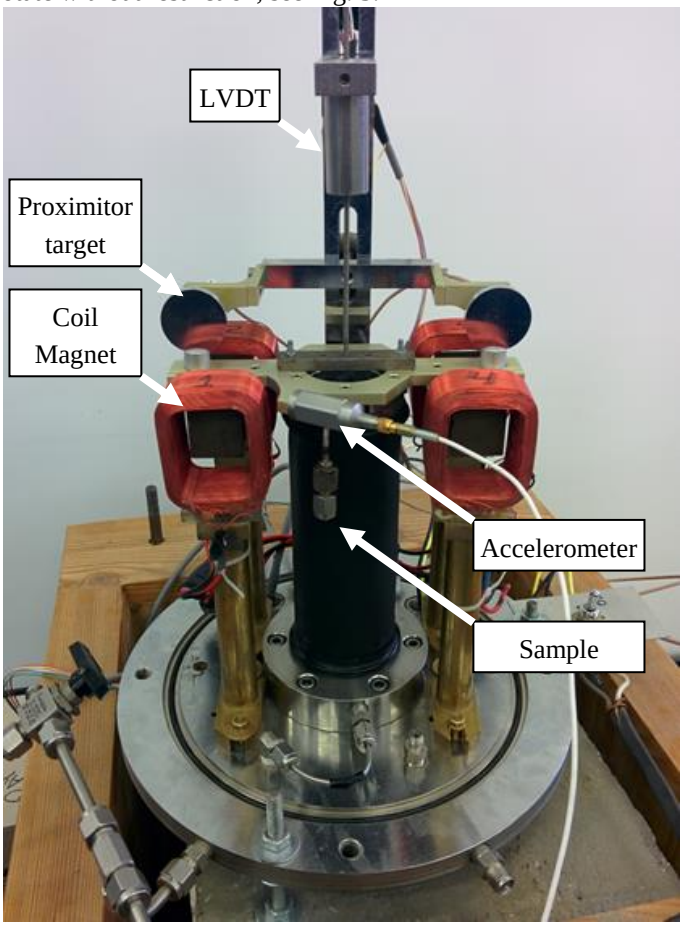

Fig. 3 Resonant Column-Torsional Simple Shear device with hollow cylinder sample

The magnets are individually surrounded by coils (in red color in Fig. 3) but they are free to move, therefore the sample is freely rotating around the vertical axis of the sample when a regulated flow of electricity in the coils causes the magnets to move. Hollow cylindrical samples are used for testing to insure a more even distribution of induced shear stresses and strains in the sample. For this comparative study, results of a combined RC-TOSS test performed on a dry sand were used. The specimen was prepared by dry pluviation from a height of 50 cm. A vacuum confinement of 84kPa was applied to the specimen during the assembly of the drive head and setup of measurement system. During the RC test, an accelerometer was used for measuring rotational acceleration of the top of the sample. For the TOSS test, a pair of proximitors measured gap distances on two steel targets fixed on the drive head. An LVDT was mounted on the support rod to determine any vertical movement during testing. Stress controlled testing was used while strain controlled testing is under development. Over 200 tests have been performed at SZE in the past several years.

Some selected results of the combined test are shown in Fig. 4 and Fig. 5.

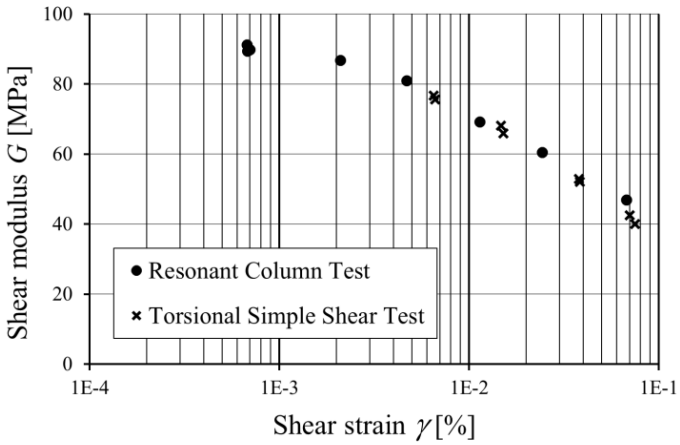

Fig. 4 Modulus reduction curve obtained with Resonant Column-Torsional Simple Shear device

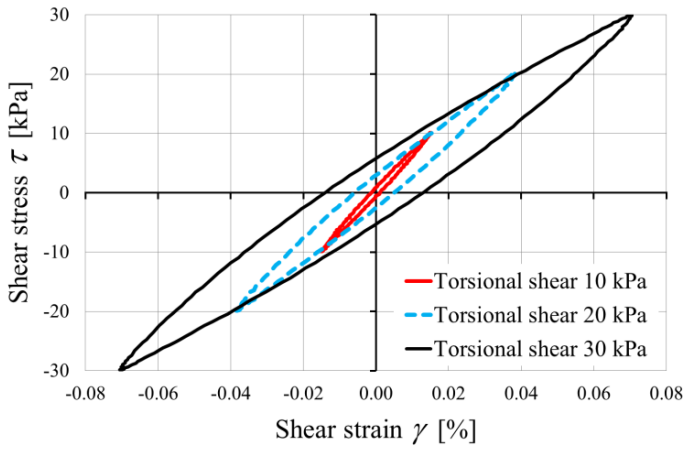

Fig. 5 Hysteresis loops of Torsional Shear tests at different stress (strain) levels

5 Modeling

5.1 General modeling aspects

Finite element modeling of such tests is a challenge. Since the setup of the test is fundamentally axisymmetric, a realistic 3D model can be generated only by software capable of

handling axisymmetric coordinate systems. An extended 2D (or 2.5D) axisymmetric model cannot be used, since the torsional load must be defined perpendicular to the model plane which is not possible.

In Midas GTS NX axisymmetric 3D modeling can be performed by either defining a global or element axisymmetric coordinate system. For this study the latter was used. Fig. 6 shows a part of the model with the finite element mesh. Hexahedral high order elements with 20 nodes were used with an average size of 4x4x3 mm. Nodes on the grey soil elements can be seen in blue in Fig. 6. This mesh was chosen so that three layers of elements would build up the cross section and so strain distribution could easily be assessed within the 1 cm thick hollow cylinder. More refined meshes were studied with little increase in accuracy.

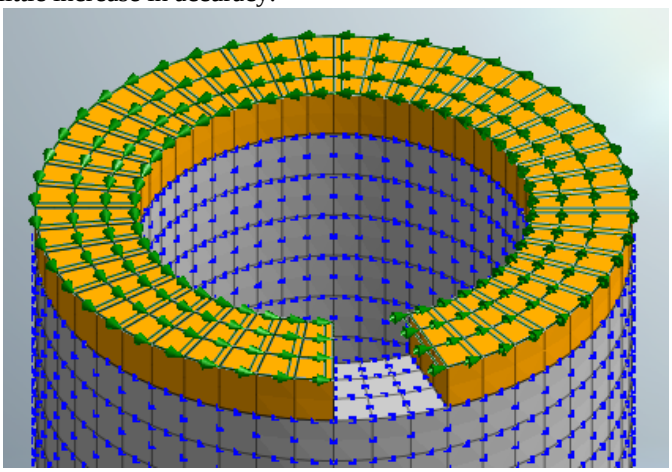

Fig. 6 Detail of finite element mesh of soil sample and steel ring (partially removed)

Fig. 6 also shows yellow elements on top of the hollow cylinder soil sample, representing the steel ring which transfers the load to the soil sample. A part of this ring is switched off to better show soil elements. The imposed torsional load is modeled as surface stress acting in the rotational direction of the axisymmetric element coordinate system. Without this option, an imposed node load would act in a continuing tangential direction which does not reflect the true loading behavior as the specimen rotates.

The mesh consisted of 4032 elements. More refined meshes showed similar results while an even a coarser mesh with one layer of high order elements with a total number of 162 elements showed identical results of overall specimen behavior.

Pinned boundary conditions were used on the bottom surface of the soil sample since in the test the soil directly connects to the rough surface of the porous stone. It should be noted that some stress irregularities were observed even in the fine mesh close to the fixity when using fixed boundary conditions (fixed against translation and rotation in each direction). The irregularities with pinned fixities were minor, see Fig. 7. Since the testing device is free on top and the self-weight of the drive head is counterbalanced by a calibrated vertical spring, no other fixities had to be applied to the model.

Calculation stages consisted of initial stress generation, confinement activation (with free face surface pressure acting in a direction normal to the outer element faces) and torsional loading stages. This can be done in the software by defining construction stage sets and setting up construction stage analysis cases. Another important modeling step is to define output control before starting the calculation. Small sub-sets of the mesh can be chosen for documenting stress, strain, etc. While the calculations were performed for the whole mesh, results were saved only for these selected elements, significantly reducing output data storage requirements. This was crucial for 3D FEM calculations since one time history result could occupy several gigabytes of storage. With such a large data set, analyzing results were slowed significantly and inevitably led to hard drive capacity issues. Result types (deformation, stress, strain) can also be set before analysis. Oddly, Midas software does not record element strains by default which can lead to some initial confusion for new users.

Formulation of the material model has been presented in Chapter 3. An additional modeling detail in Midas is that the user can specify using the model in “shear only” mode; which was done in this study. Unfortunately, the effects of this option are not detailed in the manual, however the online release notes explain that if this mode is used, shear modulus will be different in each direction separately (G_{xy}, G_{yz}, G_{zx}), otherwise an equivalent shear modulus will be used (G_{eq}). While this information is somewhat helpful, there seems to be no way of specifying shear moduli for each direction and the formulation of G_{eq} is not fully explained as of the time of modeling.

5.2 Back analysis of model parameters

Obtaining soil parameters for FEM models from various laboratory and field tests is also a challenging task. Some geotechnical FEM software even offer built-in program modules for fitting curves of commonly used laboratory tests, (e.g. Soil Test module in Plaxis), so that the user can assess the effects of changing a single parameter and chose the most appropriate set of parameters for the specific project. However laboratory tests such as the Resonant Column or Torsional Shear Test are not yet implemented in any of the mentioned modules.

For this study, in order to obtain model parameters, the G_0 value measured in low strain Resonant Column tests and the stress-strain values of a higher strain single hysteresis loop obtained with the Torsional Shear test were used. The measurement results were imported into MS Excel and the formulation of the material model was implemented into a Visual Basic code. Then, with a set of initial estimates for γ_r and h_{max} the response of the model was calculated. Due to the properties of the formulation, if a full hysteresis loop is used, the turnaround point has to be specified in advance as well.

Then for each data point the square of the error between measured and computed by the RO model could be obtained and sum of the error squares could be calculated. The MS Excel Solver module was then used to choose model parameters with the best fit. Solver uses the nonlinear GRG method (Generalized Reduced Gradient) to minimize the sum of error squares by changing the two model parameters. The obtained model parameters are summarized in Table 1.

Table 1 Ramberg-Osgood material model parameters used in this study

Parameter		Value	Dimension
Small strain stiffness from RC test	G_0	91 161	kPa
Reference shear strain*	γ_r	$8.1372*10^{-4}$	-
Max. damping constant*	h_{max}	0.19043	-
Dry density	γ_d	16.15	kN/m^3
Poisson's ratio	υ	0.3	-
**Parameters modified by Solver for obtaining best fit*			

From a practical viewpoint; the GRG method works best if the fitting parameters are of the same order of magnitude. This can be achieved by simply scaling the parameters in the formulation (e.g. using a parameter value 100x larger, and then dividing it by 100 in the formula).

6 Results

Horizontal stresses after the 84kPa confinement step are shown in Fig. 7. Some minor irregularities can be observed close to the base fixities. However, the difference is less than 1%.

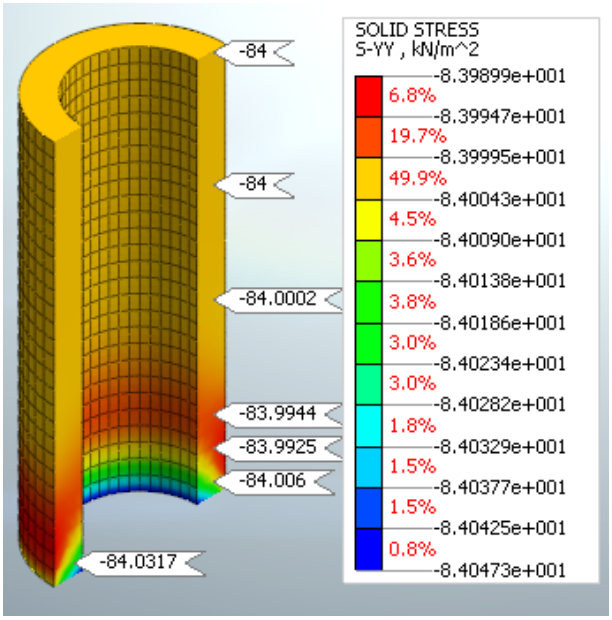

Fig. 7 Distribution of horizontal normal stresses after confinement activation

A one-way loading stress-strain curve is shown in Fig. 8. Stress and strain values were taken as the average of three layers of elements in the cross section. This average was found to be almost identical to the value in the middle element. Agreement between the formulation and the FEM calculation is nearly exact.

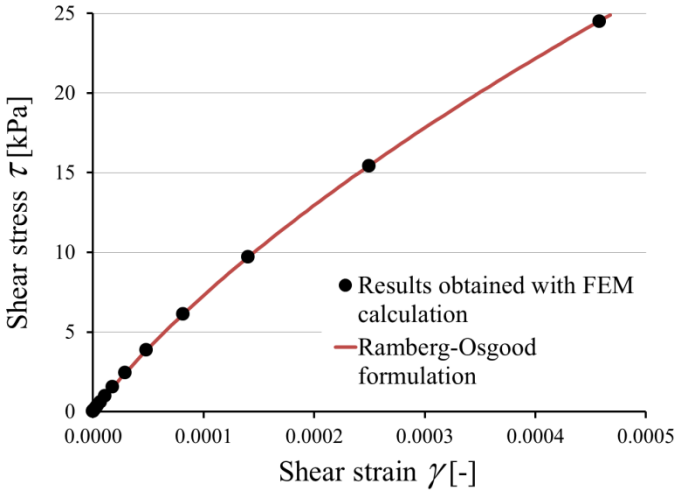

Fig. 8 Stress-strain curve by FEM calculation and MIDAS Ramberg-Osgood formulation

Fig. 9 and Fig. 10 show the deformed mesh and the distribution of total deformations in the mesh. The horizontal shear of the elements is clearly observable.

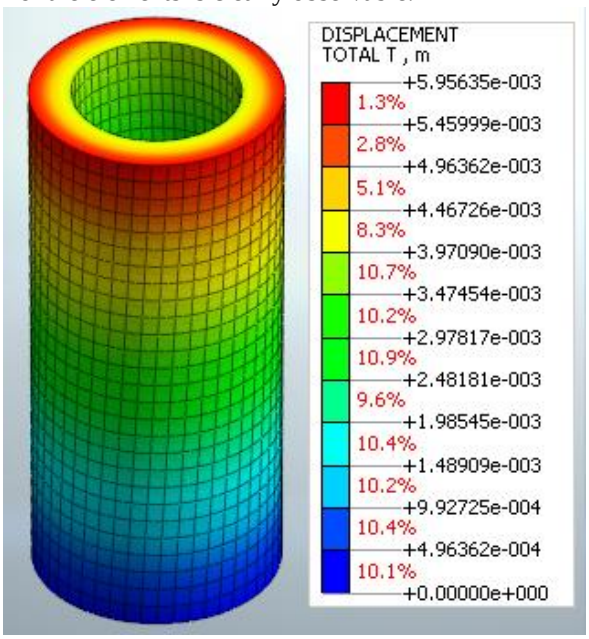

Fig. 9 Deformed mesh at turnaround point of loading

As expected, the top of the soil cylinder moves the most, while there is no movement at the fixity. The cross section also reveals that displacement distribution is also realistic in any horizontal plane, namely there is larger displacement at the outer rim of the cylinder than at the inner rim.

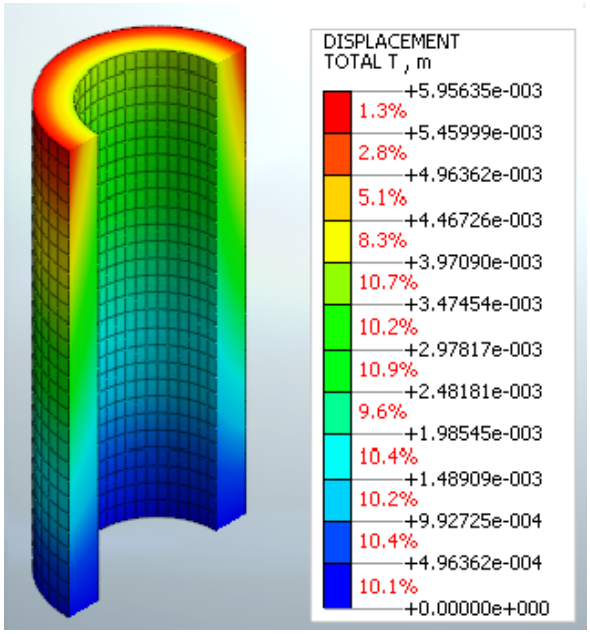

Fig. 10 Distribution of total displacements at turnaround point of loading

Fig. 11 shows shear strain distribution in the sample, which is even throughout the height of the sample. Also the benefit of using a hollow cylinder for testing is demonstrated here; strain difference within the sample (±20% of average) would be considerably higher in a solid cylinder.

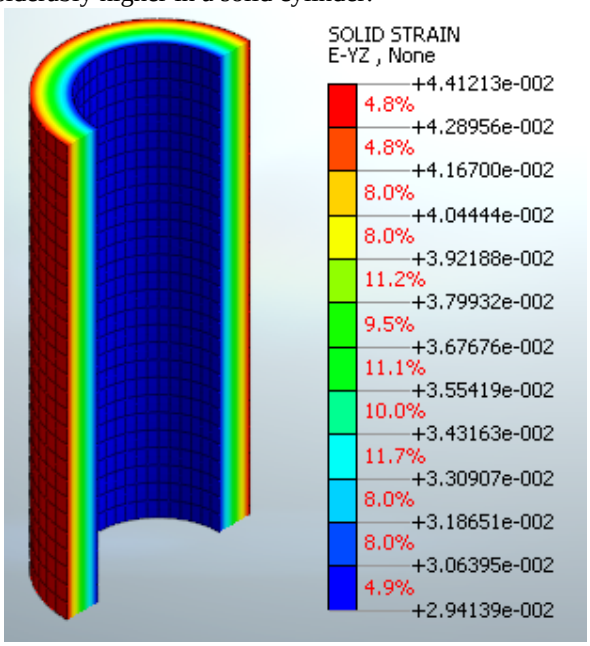

Fig. 11 Shear strain distribution at turnaround point of loading

The calculations were performed at several shear strain levels and based on the obtained shear stress and strain values; the secant shear modulus was calculated. Fig. 12 shows the normalized modulus degradation curve compared to the test data.

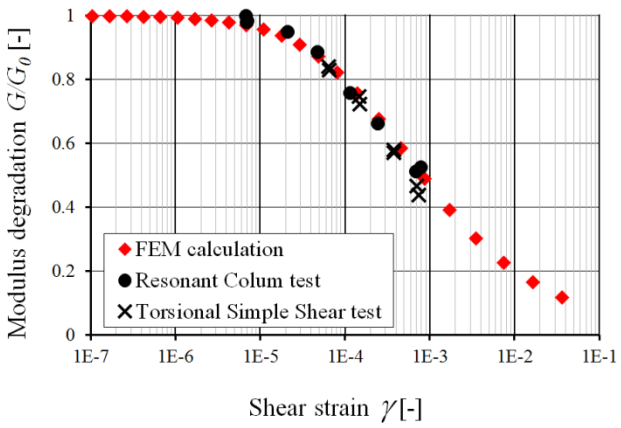

Fig. 12 Modulus reduction curve by FEM calculation and RC-TOSS tests

7 Conclusions

This study verified that the Ramberg-Osgood material model implemented in MIDAS GTS NX v2014 is capable of modeling this static axisymmetric laboratory test with representation of nonlinear material behavior. Modulus degradation and hysteretic behavior was also captured by the model. Future studies will focus on modeling dynamic tests.

References

[1] Brinkgreve, R. and Engin, E. "Validation of geotechnical finite element analysis," in *Proceedings of the 18th International Conference on Soil Mechanics and Geotechnical Engineering*, Paris, France, ISSMGE TC 103, 2013, pp. 677-682. http://www.issmge.org/uploads/publications/1/2/677-682.pdf.

[2] Richart, F.E. Jr. "Some Effects of Dynamic Soil Properties on Soil-Structure Interaction," in *Journal of the Geotechnical Engineering Division, 101*(12), 1975, pp. 1193-1240. http://cedb.asce.org/CEDBsearch/record.jsp?dockey=0006358.

[3] Atkinson, J.H. and Sallfors, G. "Experimental determination of soil properties," in *Proceedings of the 10th European Conference on Soil Mechanics and Foundation Engineering Vol 3*, Florence, 1991, pp. 915-956.

[4] Clayton, C.R.I. "Stiffness at small strain: research and practice," in *Géotechnique 61*, No.1, 2011, pp. 5-37 https://doi.org/10.1680/geot.2011.61.1.5.

[5] MIDAS Information Technology Co., „Midas GTS NX 2014 v2.1 Analysis Reference, Chapter 4. Materials," 2014, pp. 105-211. http://midasgtsnx.com/.

[6] Ramberg, W. and Osgood, W.R. "Description of stress strain curves by three parameters," in *National Advisory Committee for Aeronautics, Technical Note No. 902*., 1943, p. 28. http://hdl.handle.net/2060/19930081614.

[7] Streeter, V.L, Wylie, E.B, Richart, F.E.Jr. "Soil Motion Computation by Characteristics Method" in *Journal of the Geotechnical Engineering Division, Vol.100*, No.GT3,

1974, pp. 247-263.

[8] Ishihara, K. „*Soil Behavior in Earthquake Geotechnics*” New York, Oxford University Press, 1996, pp. 33-39. ISBN 0-19-856224-1.

[9] Adachi N. and F. Tatsuoka, „*Soil mechanics III-consolidation, shear and dynamic analysis*” Gihodo, Tokyo, 1986, pp. 1-339.

[10] Ray, R.P. and Woods, R. „Modulus and damping due to uniform and variable cyclic loading,” in *Journal of Geotechnical Engineering 114.8*, American Society of Civil Engineers, 1988, pp. 861-876.

http://dx.doi.org/10.1061/(ASCE)0733-9410(1988)114:8(861)#sthash.KY9d5G8T.dpuf.

[11] Ray, R.P. "*Changes in shear modulus and damping in cohesionless soils due to repeated loading*, PhD Dissertation," Michigan, USA, University of Michigan, 1983, p. 417.

[12] Ray, R. P., Szilvágyi, Z., "Measuring and modeling the dynamic behavior of Danube Sands," in *Proceedings 18th International Conference on Soil Mechanics and Geotechnical Engineering: Challenging and Innovations in Geotechnics*, Paris, Presses des Ponts, 2013, pp. 1575-1578.

http://www.cfms-sols.org/sites/default/files/Actes/1575-1578.pdf.

[13] Szilvágyi, Z., Hudacsek P., Ray, R.P, "Soil shear modulus from Resonant Column, Torsional Shear and Bender Element Tests," in *International Journal of Geomate 10*:(2), 2016, pp. 1822-1827.

http://www.geomatejournal.com/node/367

[14] Szilvágyi, Zs., Panuska, J., Kegyes-Brassai, O., Wolf, Á., Tildy, P., Ray, R.P., "Ground Response Analyses in Budapest Based on Site Investigations and Laboratory Measurements," in *International Journal of Environmental, Chemical, Ecological, Geological and Geophysical Engineering Vol:11, No 4*, World Academy of Science Engineering and Technology, 2017, pp. 307-317 http://scholar.waset.org/1999.6/10006887.